Int. J. Electrochem. Sci., 15 (2020) 9543 – 9553, doi: 10.20964/2020.08.56

International Journal of
ELECTROCHEMICAL
SCIENCE
www.electrochemsci.org

Short Communication

Preparation of MOF Derived Zn-Co-C Composite as Anode for Lithium-ion Batteries

Mingyuan Ren[1], *Honghai Xu*[2], *Guoxu Zheng*[1], *Xiaowei Han*[3,*]

[1] School of software and microelectronics, Harbin University of Science and Technology, Harbin 150080, P. R. China
[2] School of science, Harbin University of Science and Technology, Harbin 150080, P. R. China
[3] School of Computer and Information Engineering, Harbin University of Commerce, Harbin 150028, P. R. China
[*]E-mail: hanxiaowei2017@163.com

Received: 22 January 2020 / *Accepted:* 9 May 2020 / *Published:* 10 August 2020

This paper focuses on the preparation of hollow mixed metal oxide materials by means of mixed metal atom doping. In this paper, the hollow core-shell structure Zn-Co-MOFs material was prepared by hydrothermal method, calcined into Zn-Co-C material, and its conductivity and electrochemical performance were improved on the basis of retaining hollow core-shell channel structure. Hollow core-shell structure to avoid direct contact with the electrode materials and electrolyte, reduce the electrolyte decomposition, a loop to form porous channel structure, shorten the lithium ion diffusion path and improve the lithium storage capacity, core-shell structure ACTS as a skeleton structure, effectively relieve internal stress changes, the structure of the electrode material volume change and destruction, reduce capacity attenuation. The Zn-Co-C composite has a discharge specific capacity of 1749mAh g^{-1} in the first coil and a maximum coulomb efficiency of 99.8%. At 200 mA g^{-1} current density, the reversible capacity is up to 704mAh g^{-1} at 200 cycles, and the multiplier and impedance are also excellent.

Keywords: MOFs, Mixed metal oxide, LIBs, electrode materials

1. INTRODUCTION

As an efficient and stable energy storage device, lithium ion battery (LIBs) has become an important part of today's society and is widely used in production and life. Research on the performance of LIBs has also received extensive attention from researchers. As the electrode material that plays a decisive role in battery performance, we focus on the research object. Metal organic framework (MOFs) is a kind of coordination polymer that has attracted extensive attention in recent years [1-2]. With MOFs as the forebody, porous metal oxides and porous carbon materials with controllable structure can be obtained. As an electrode material, it can significantly improve the

electrochemical performance of batteries. MOFs has become the material of choice for our new electrode materials. In contemporary society, with the depletion of non-renewable energy reserves and the destruction of the ecological environment, the development of green new energy is increasingly valued by us. As one of the important equipment for energy storage, LIBs is widely used in our production and life [3-5]. The electrochemical properties of LIBs are mainly determined by the electrode materials, and nanostructured materials with high theoretical capacity are proposed as the electrode materials, so as to present excellent electrochemical properties [6-9]. As a new kind of electrochemical functional materials, MOFs have many unique advantages, such as very large specific surface (the largest specific surface is close to the maximum calculated by solid theory), regular and rigid channel structure, channel size adjustable, structure designability, etc. MOFs materials have been paid more and more attention by researchers both at home and abroad. Its structure is generally composed of organic ligand and metal ions self-assembled at the appropriate solvent temperature into a three-dimensional ordered networklike crystal. In order to give MOFs more functions and characteristics, a lot of efforts have been made to construct composite materials of metals and their compounds with MOFs, such as metal elements, metal oxides, etc [10-12]. Recently, metal nanoparticle @MOFs composite material has shown unique advantages in many new catalysis, so it has gradually become a star material [13-14]. For example, encapsulating metal nanoparticles in MOFs can effectively prevent agglomeration and improve their thermal stability [15-16]. Mixed transition metal oxides can provide more kinds of active substances and abundant redox reactions than single transition metal oxides. By virtue of its internal space structure, the hollow structure composite material can effectively alleviate the volume change and structure damage of the electrode material during the charge-discharge cycle. Based on the above studies, a special hollow polyhedron core-shell channel structure was constructed in this paper. Under hydrothermal reaction, phase transformation of MOFs material occurred to obtain hollow Zn-Co-MOFs material. Under calcination condition, organic ligand bonding metal center of mixed MOFs precursor material was directly transformed into hollow porous core-shell structure Zn-Co-C composite material. As a cathode material for lithium ion batteries, excellent electrochemical properties can be obtained.

2. EXPERIMENTAL

2.1 Preparation of ZIF-8

The preparation steps of the precursor ZIF-8 are as follows :(1) weigh 0.7344g of zinc hexahydrate, dissolve it in 50ml of methanol, stir it thoroughly, and get solution A. (2) 0.8106g of 2-methylimidazole and 0.6715g of sodium formate were weighed, dissolved in 50ml of methanol, and stirred thoroughly to obtain solution B. (3) pour solution B into solution A and stir thoroughly at room temperature for 24 hours. After washing with methanol, ZIF-8 was obtained by vacuum drying.

2.2 Preparation of Zn-Co-MOFs and Zn-Co-C

The preparation steps of Zn-Co-MOFs and Zn-Co-C are as follows :(1) weigh zif-8 of 0.08g and dissolve it in 10ml of methanol to obtain solution C. (2) 0.2417g of cobalt hexahydrate and 0.895g

of 2-methylimidazole were weighed and dissolved in 6ml of methanol, respectively, to obtain solutions D and E. (3) add solution D and E to solution C, stir them thoroughly, pour them into the reaction kettle and put them into the oven. The temperature is set to 120℃ and the reaction time is set to 4h. (4) remove the reactor, cool it naturally to room temperature, wash it with ethanol, dry it, and finally get Zn-Co-MOFs. The prepared Zn-Co-MOFs material was put into muffle furnace and calcined at 350℃ for 2h to obtain Zn-Co-C. According to the weight of the weighed drugs, the molar ratio of Zn-Co-C is 1 :1 :10. The preparation flow chart is shown in figure 1.

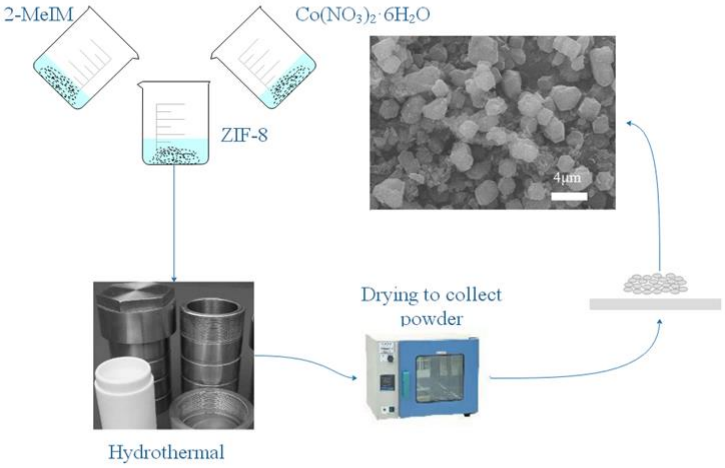

Figure 1. Schematic diagram

2.3 Materials characterization

Material characterization tests were performed by X-ray diffraction (XRD) and scanning electron microscopy (SEM).

2.4 Electrochemical measurements

An electrode sheet was prepared, and the prepared electrode material, Super-P carbon black (conductive additive) and polyvinylidene fluoride (PVDF) were uniformly stirred with N-methylpyrrolidone (solvent) in a ratio of 8:1:1 to prepare a suspension. Next, the suspension was evenly dispersed on a circular copper piece, and a button battery (CR2302) was assembled in an argon-filled glove box. Finally, the electrochemical performance was tested.

3. RESULTS AND DISCUSSION

As can be clearly seen from figure 2(a-b), the diameter of Zn-Co-MOFs material is about 2-3μm. Zn-Co-MOFs materials are uniformly dispersed and closely packed. The surface is smooth and has clear channels. It is because of this multi-channel structure that Zn-Co-MOFs material can absorb

more lithium as electrode material and has better electrochemical performance. In figure 2(c-d), it can be clearly seen that Zn-Co-C material is evenly distributed, and the advantages of multi-channel surface of Zn-Co-MOFs material are retained. The structure of the hollow core shell is clearly seen by TEM (e-f).

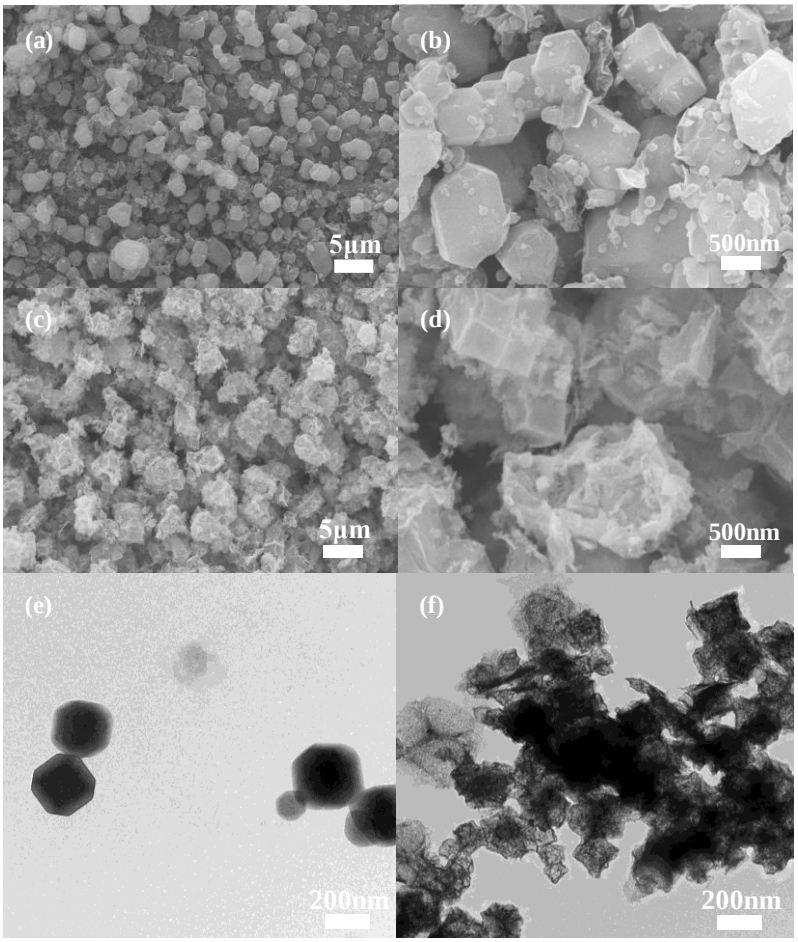

Figure 2. SEM images of (a-b) Zn-Co-MOFs, (c-d) Zn-Co-C; TEM images of (e) Zn-Co-MOFs, (f) Zn-Co-C

Figure 3 shows the XRD patterns of Zn-Co-MOFs and Zn-Co-C samples. The diffraction peaks of Zn-MOFs, Co-MOFs and Zn-Co-MOFs are basically the same. Since they have similar lattice constants and crystal structures, the Co-MOFs shell can be ensured to grow evenly on the Zn-MOFs surface. The three diffraction peaks are strong and sharp, indicating good crystallinity. The diffraction peaks of Zn-Co-C are similar to those obtained by X-ray diffraction of Zn and Co. Therefore, Zn-Co-C materials have been successfully synthesized.

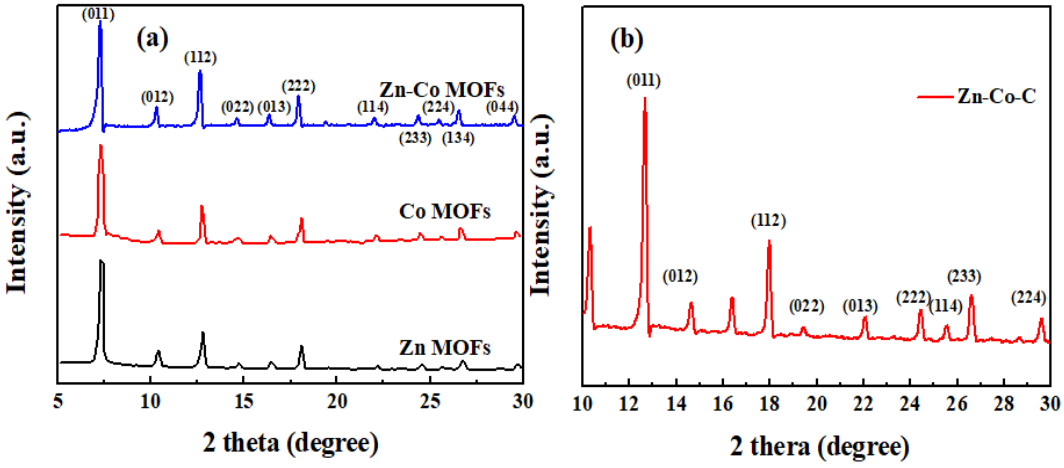

Figure 3. XRD patterns of (a) Zn-Co-MOFs, (b) Zn-Co-C

In order to study the electrochemical behavior of electrode materials during charge and discharge, a new battery with Zn-Co-C electrode was tested.

Figure 4 is the CV curve of the new battery with Zn-Co-C material as the electrode. In the figure, it can be clearly seen that during the first cycle of discharge, there are two obvious reduction peaks at 0.27v and 0.51v, and a small reduction peak at 1.25v. The larger reduction peak at 0.27v corresponds to the reduction of Zn^{2+} to Zn in the discharge process, while the smaller reduction peak at 0.51v and the very small reduction peak at 1.25v correspond to the multi-step reduction of cobalt ions to Cobalt in the discharge process. Meanwhile, the reduction of Zn^{2+} to Zn is accompanied by the formation of solid electrolyte interface membrane (SEI membrane), and the process is irreversible [17-19]. During the first charging cycle, there was an obvious oxidation peak at 1.6v and a very small one at 0.7v. The oxidation peak of 0.7V corresponds to the oxidation of Zn to Zn^{2+}, and the oxidation peak of 1.6V corresponds to the generation process of cobalt ions [20]. Due to the formation of the SEI film, the battery capacity is irreversibly reduced, and at the same time, the interface resistance between the electrode and the electrolyte is increased, which affects the battery's charge and discharge performance. But the formation of SEI film has another advantage, it can prevent the organic electrolyte from further reaction with the material, improve the cycle efficiency and reversible capacity of the battery[21-23] .Compared with the first cycle, the range of oxidation peak and reduction peak in the second cycle is significantly smaller than that in the first cycle, and the reduction peak shifts to the right to some extent. The integral area is also significantly smaller than the first circle. In the second cycle of discharge, there is a relatively obvious reduction peak at 0.7v, corresponding to the reduction of Zn^{2+} to Zn, accompanied by the reduction of Co^{2+} to Co, while the reduction peak of cobalt ions in other valence states to cobalt is not detectable. Reduction in the number of oxidation and reduction peaks Co ions form, the main reason is that can form a variety of valence state of cobalt element, but on the first lap after discharge reduction of cobalt, charging with electrolyte of Co ion valence mostly Co^{2+}, so after the first lap circle of charging and second charge and discharge process, the other Co ion valence state of redox peaks can be found out. It can be clearly seen from the figure that the redox process in the third circle is similar to that in the second circle. Both oxidation peak and reduction peak

are close to those in the second circle, and the integral area does not decrease significantly. The closer the peak position of the oxidation peak and the reduction peak, the sharper the shape, the less obvious the polarization phenomenon during the charging and discharging of the lithium ion battery, and the better the electrochemical performance of the battery [24].

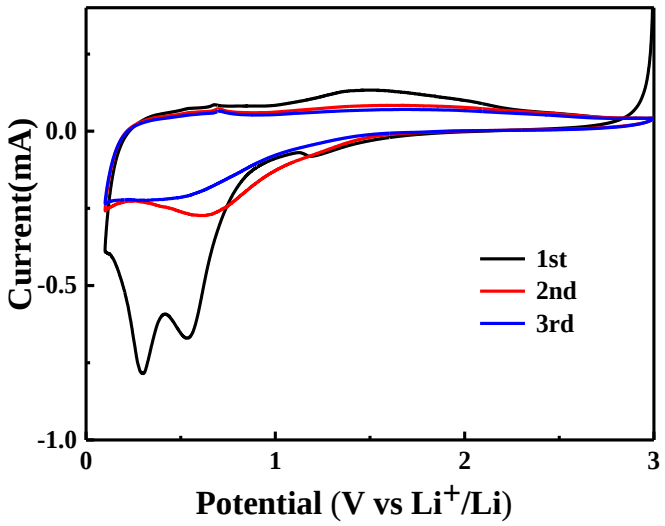

Figure 4. cyclic voltammetry curve of Zn-Co-C

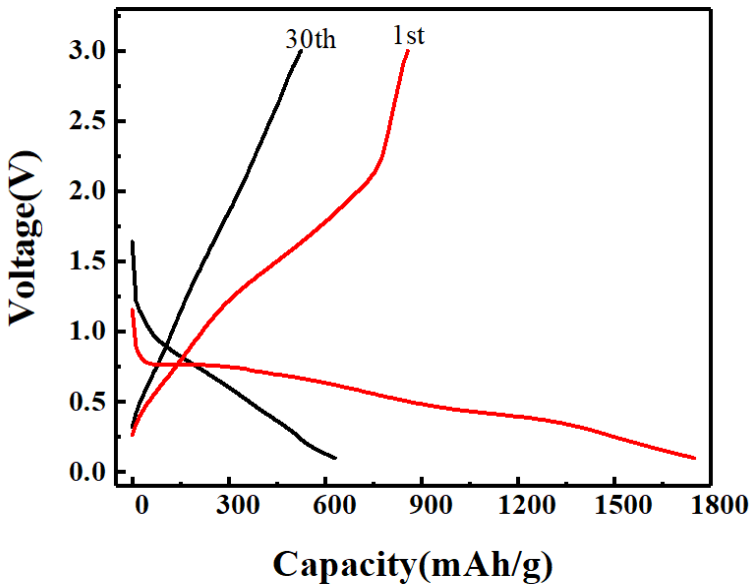

Figure 5. charging and discharging curves of Zn-Co-C

Figure 5 shows the charge-discharge curve of Zn-Co-C. As can be clearly seen from the figure, for the lithium ion battery assembled by Zn-Co-C material, its first discharge specific capacity is 1749mAh g^{-1}, and the first charge specific capacity is 858mAh g^{-1}, and the corresponding first coulomb efficiency is 49.03%. In the next charging and discharging cycle, the specific capacity rapidly

attenuates. In the thirtieth cycle, the discharge specific capacity is about 630mAh g^{-1}, and the charging specific capacity is about 525mAh g^{-1}, but its coulomb efficiency rapidly increases to 83.26%. During the first discharge, the voltage drops rapidly to the voltage platform of about 0.7, and then slowly drops to the cut-off voltage of 0.01v. This curve is basically consistent with the results obtained in the cyclic voltammetry test. At this point, the corresponding reduction process of Zn^{2+} to Zn is accompanied by the formation of SEI membrane. Because of the SEI membrane, the specific capacity of the 30th charge and discharge decreased obviously, and the voltage of the subsequent discharge platform increased obviously. These results are consistent with those obtained by cyclic voltammetry.

In order to test the specific capacity attenuation and coulomb efficiency of Zn-Co-C lithium ion battery after multiple cycles, Zn-Co-C lithium ion battery was charged and discharged for 200 cycles at the current density of 200mA g^{-1} between 3.00v and 0.01v. The result is shown in figure 6. The discharge specific capacity of the Zn-Co-C lithium ion battery reached 1749mAh g^{-1} in the first lap, but dropped rapidly in 1-15 laps. The discharge specific capacity in the 15th lap was only 754mAh g^{-1}. After the 15th lap, it tends to be stable and the descent is relatively slow. It reaches the lowest point in the 99th lap, which is only 493mAh g^{-1}. However, it starts to recover slowly compared with the capacity in the 100th lap and rises to 704mAh g^{-1} in the 200th lap. The specific discharge capacity of Zn-Co-C lithium ion battery decreased rapidly in the first 15 laps, partly because the SEI film greatly reduced the capacity of lithium ion battery during the first several charging and discharging processes, and the process was irreversible. Another part of the reason for that, in the process of charging and discharging lithium ion between the electrode materials embedded in and out, part of the lithium ion after embedding, due to the structure and the cause of the electrode materials and electrolyte contact area, failed to emerge, resulting in a decrease of the number of lithium ion in the electrolyte of slow, results in the decrease of lithium ion battery capacity of slow, this part of the reason is caused on lap 15-100 battery capacity of the main causes of slow decline. But in 100, after the battery discharge specific capacity of the slow rebound, the main reason is that the structure of the electrode material nested Li_2O tends to be stable, and electrode materials and electrolyte contact more fully, in the process of lithium ion out, not only can emerge in all types of lithium ion, also can have a part in 1-100 lap embedded lithium ions can also emerge from the electrode material, causing an increase in the number of lithium ion in the electrolyte, lithium ion battery discharge specific capacity slowly lift [25-27]. Zn-Co-C assembly materials of lithium ion battery in the first lap of coulomb efficiency is only 49.03%, but in 1-15 laps rapidly increases, the 15th lap coulomb efficiency has reached 95.41%, and starting from 35 laps, Zn-Co-C material construction of the coulomb efficiency lithium ion batteries are not less than 98%, and the highest when the coulomb efficiency reached 99.8%, 50% - 70% of the coulomb efficiency compared to other materials, Zn-Co-C material assembly of reversible performance of lithium ion battery was better than other batteries, and the performance is very good.Table.1 Comparison of cycle performance of Zn-Co-C materials with other Zn-Co-C materials with different morphologies.

Table 1. Comparison of cycle performance of Zn-Co-C with other bimetal oxides

Zn-Co-C	200mA/g	704mAh/g after 200 cycles	This work
Zn-Co-C	2000mA/g	486mAh/g after 40 cycles	This work
$ZnCo_2O_4$	2000mA/g	399mAh/g after 20 cycles	[28]
$ZnCo_2O_4$ nanoparticles	450mA/g	378.1mAh/g after 70 cycles	[29]
$ZnCo_2O_4$ microspheres	1000mA/g	432mAh/g after 40 cycles	[30]

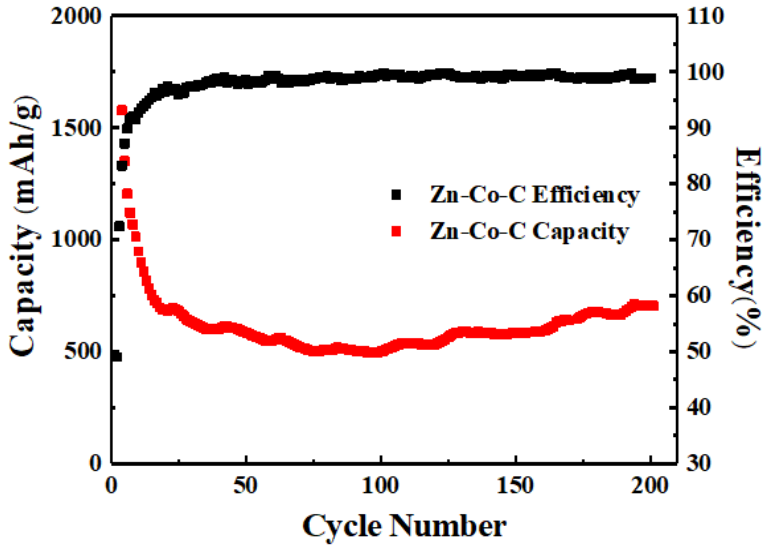

Figure 6. cyclic performance curves of Zn-Co-C

The lithium ion battery electrode voltage at 0.01 V to 3.00 V, current density were 0.2 C, 0.4 C and 0.8 C and 1.2 C, 1.6 C and 2.0 C finally returned to 0.2 C, the result is shown in figure 7, Zn-Co-C lithium ion battery charging and discharging rate, excellent performance under the current density of 1.2 C, the capacity in a 486mAh g^{-1}, under the high current density of 2 C, capacity remains in 240mAh g^{-1} when current density back to 2 C, Zn-Co-C discharge specific capacity to recover to 1749mAh g^{-1}, It indicates that the composite material has good cyclic stability. The excellent multiplier performance is attributed to the hollow core shell structure providing more active sites, increasing the contact area between the electrode and the electrolyte, and improving the electrochemical activity of the composite. The cavity structure provides buffer space for the change of electrode material volume to ensure the structure stability.

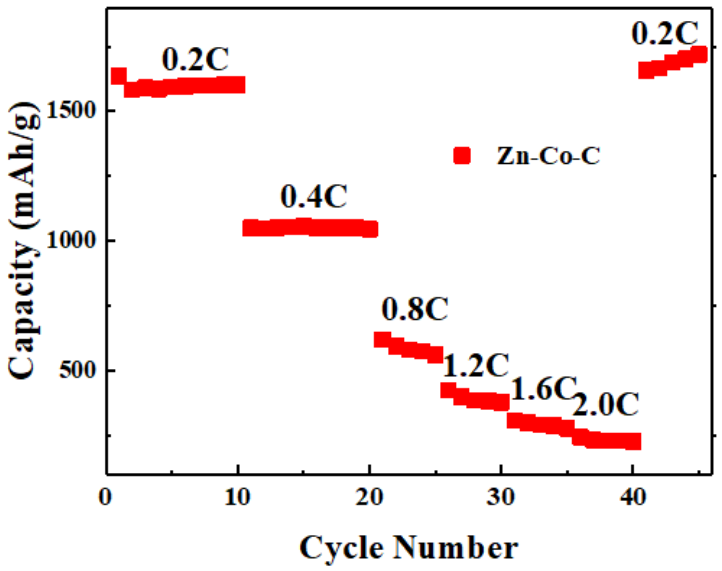

Figure 7. cyclic performance curves of Zn-Co-C

Figure 8 shows the ac impedance test results of Zn-Co-C lithium ion battery. The AC impedance curve of the battery is mainly composed of two parts: the half arc in the high frequency area and the oblique line in the low frequency area.

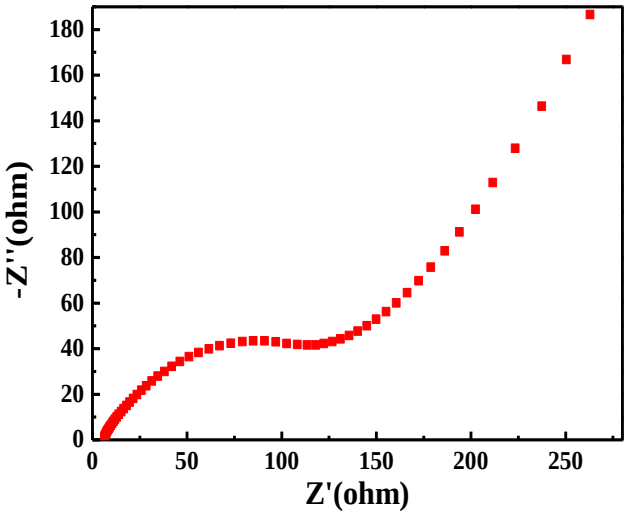

Figure 8. AC impedance sectroscopy of Zn-Co-C

The semicircle in the high frequency region corresponds to the charge transfer between the SEI film and the active material interface, while the semicircle diameter, the charge transfer resistance of the reaction sample, and the oblique line in the low frequency region indicate the diffusion of lithium ion in the electrode material. The smaller the slope, the weaker the diffusion capacity, and the ideal state is when the slope of the oblique line is 1[31]. The figure shows the lower impedance and higher charge transfer efficiency of Zn-Co-C lithium ion batteries. This is mainly because the porous hollow

structure can effectively shorten the diffusion path of lithium ions and reduce the diffusion resistance of lithium ions. In addition, the two metal oxides combine to enhance the ability of charge transfer. The composite structure with porous channels can enlarge the pores and increase the specific surface area of electrochemical activity. When the electrode surface reaches the ideal aperture distribution, the diffusion resistance of lithium ions decreases and the linear slope in the low-frequency area is larger.

4. CONCLUSIONS

The Zn-Co-C composite prepared in this paper has a core-shell particle composite structure with particle size of 2-3 μm. The Zn-Co-C composite has a discharge specific capacity of 1749mAh g^{-1} in the first coil and a maximum coulomb efficiency of 99.8%. At 200mA g^{-1} current density, the reversible capacity is up to 704mAh g^{-1}, 2C high current density, and the discharge specific capacity is maintained at 240mAh g^{-1} when the cycle is in 200 cycles. The porous channel structure is formed in the circulation to shorten the diffusion path of lithium ions and improve the embedded release speed and storage capacity of lithium ions. Core-shell structure as the skeleton structure, effectively relieve internal stress changes, the structure of the electrode material volume change and destruction and so on. The electrode material also contributes a wealth of zinc and cobalt ions, and more redox reactions will occur during charge and discharge, and more charge discharge processes will occur, improving the diffusion performance of lithium ions in the active material, thereby significantly improving the material Electrochemical performance [32]. When Zn-Co-C is used as the electrode of lithium ion battery, it presents excellent characteristics and is an excellent material used as the electrode of lithium ion battery. Its stable cycling performance guarantees the battery life, is a new type of green energy, can become a high specific volume and excellent cycling performance of electrode materials.

ACKNOWLEDGMENTS
This work was supported by the Fundamental Research Foundation for Universities of Heilongjiang Province (Grant No. LGYC2018JC018), and supported by the Heilongjiang Province Natural Science Foundation (Grant No. F2018020).

References

1. X. Xu, W. Shi, P. Li, S. Ye, C. Ye, H. Ye, T. Lu, A. Zheng, J. Zhu, L. Xu, M. Zhong and X. Cao, *Chem. Mater.*, 29 (2017) 6058-6065.
2. X. Cao, C. Tan, M. Sindoro and H. Zhang, *Chem. Soc. Rev.*, 46 (2017) 2660-2677.
3. Y. B. Cao, F. L. Yuan, M. S. Yao, J. H. Bang and J. H. Lee, CrystEngComm, 16 (2014) 826-833.
4. K. Y. Zou, Y. C. Liu, Y.F. Jiang, C. Y. Yu, M. L. Yue and Z. X. Li, *Inorg. Chem.*, 56 (2017) 6184−6196.
5. Y. Wang, Y. Song and Y. Xia, *Chem. Soc. Rev.*, 45 (2016) 5925−5950.
6. L. Q. Sun, R. H. Cui and A. F. Jalbout, *J. Power Sources*, 189.1 (2009) 522-526.
7. J. Kim, H. Ma, H. Cha, H. Lee, J. Sung, M. Seo, P. Oh, M. Park and J. Cho, *Energ. Environ. Sci.*, 11 (2018) 1449-1459.
8. M. Chen, D. Chao, J. Liu, J. Yan, B. Zhang, Y. Huang, J. Lin and Z.X. Shen, *Adv. Funct. Mater.*, 27 (2017) 1606232.

9. M. Chen, J. Liu, D. Chao, J. Wang, J. Yin, J. Lin, H.J. Fan and Z.X. Shen, *Nano Energy*, 9 (2014) 364-372.
10. B.H. Wu and N.F. Zheng, *Nano Today*, 8(2013) 168-197.
11. Y. Wu, D.S. Wang, X.B. Chen, G. Zhou, R. Yu and Y.D. Li, *J. Am. Chem. Soc.*, 135(2013) 12220-12223.
12. N.A. Liu, Y. Yao, J.J. Cha, M.T. McDowell, Y. Han and Y. Cui, *Nano Research*, 5(2012) 109-116.
13. G. Lu, S.Z. Li, Z. Guo, O.K. Farha, B.G. Hauser, X.Y. Qi, Y. Wang, X. Wang, S.Y. Han and X.G. Liu, *Nature chem.*, 4(2012) 310-316.
14. H.R. Moon, D.W. Lim and M.P. Suh, Chem. *Soc. Reviews*, 42(2013) 1807-1824.
15. H. Khajavi, H.A. Stil and H.P.C.E. Kuipers, *Acs. Catalysis*, 3(2013) 2617-2626.
16. C. Hou, G. Zhao and Y. Ji, *Nano Research*, 7(2014) 1364-1369.
17. X. Li, D. Geng and Y. Zhang, *Electrochem. Commun.*, 8(2011) 822-825.
18. Q. Xie, F. Li and H. Guo, *Appl. Mater. Inter.*, 5(2013) 5508-5517.
19. S.Y. Tian, G.X. Zheng, Q. Liu, M.Y. Ren, J.H. Yin, *Int. J. Electrochem. Sci.*, 14(2019) 9459-9467.
20. G.X. Zheng, M.H. Chen, J.H. Yin, H.R. Zhang, X.Q. Liang and J.W. Zhang, *Int. J. Electrochem. Sci.*, 14(2019) 2345-2362.
21. R. Demir, Y.S. Hu and M. Antonietti, *Chem. Mater.*, 20(2008) 1227-1229.
22. H. Wang, L.F. Cui and Y. Yang, *J. Am. Chem. Soc.*, 132(2010) 13978-13980.
23. B. Liu, J. Zhang and X. Wang, *Nano lett.*, 12(2012) 3005-3011.
24. Y. Zhu and C. Wang, *J. Phys. Chem. C.*, 115(2010) 823-832.
25. B. Liu, J. Zhang and X.F. Wang, *Nano lett.*, 12(2012) 3005-3011.
26. B. Jin, A.H. Liu and G.Y. Liu, *Electrochim. Acta*, 90(2013) 426-432.
27. Y,R, Liu, J. Bai and X.J. Ma, *J. Mater. Chem.*, 2(2014) 14236-14244.
28. H. Zeng and Q. Wang, *Chinese Battery Industry*, 23(2019) 176-179.
29. A.K. Rai, T.V. Thi and B.J. Paul, *Nano Energy*, 11(2015).
30. L. Hu, B. Qu and C. Li, *J. Mater. Chem. A.*, 18(2013) 5596.
31. M. Winter and R.J. Brodd, *Chem. Reviews*, 104(2004) 4245-4269.
32. M. Armand and J.M. Tarascon, *Nature*, 451(2008) 652-657.